Investigation of the coupling potential by means of *S*-matrix inversion

I. Boztosun
Department of Physics, Erciyes University, Kayseri, Turkey

R. S. Mackintosh
Department of Physics, Open University, Milton, Keynes, United Kingdom
(Received 22 August 2002; published 4 December 2002)

We investigate the inelastic coupling interaction by studying its effect on the elastic scattering potential, as determined by inverting the elastic scattering *S* matrix. We first address the effect upon the real and imaginary elastic potentials of including excited states of the target nucleus. We then investigate the effect of a recently introduced coupling potential that has been remarkably successful in reproducing the experimental data for the $^{12}C+^{12}C$, $^{12}C+^{24}Mg$, and $^{16}O+^{28}Si$ reactions over a wide range of energies. This coupling potential has the effect of deepening the real elastic potential in the surface region, thereby explaining a common feature of many phenomenological potentials. It is suggested that one can relate this deepening to the superdeformed state of the compound nucleus ^{24}Mg.

DOI: 10.1103/PhysRevC.66.064602 PACS number(s): 24.10.Eq

I. INTRODUCTION

In this paper we investigate the coupling potential that gives rise to inelastic scattering by studying the total elastic scattering potential that arises in the presence of inelastic scattering. We do this by determining, by means of $S_l \rightarrow V$ inversion, the total elastic scattering potential corresponding to the elastic scattering *S* matrix. This allows us to identify the dynamical polarization potential (DPP) and it is the properties of this which we can then relate to the characteristics of the coupling potential.

Boztosun and Rae [1] have recently made a detailed analysis of the $^{12}C+^{12}C$ system over a wide energy range, and have shown that the standard (conventional) coupled-channel calculations are unable to explain the elastic and the inelastic scattering data simultaneously and that the magnitude of the mutual-2^+ cross section is underpredicted by a large factor in the $^{12}C+^{12}C$ system. This has been a major problem for the past couple of decades, but a new coupling potential proposed by these authors solves many of these problems. This new coupling potential also successfully explains elastic and inelastic scattering of the $^{12}C+^{24}Mg$ and $^{16}O+^{28}Si$ systems over a very wide range of energies [2–4].

Substantial information about the effect of this new coupling potential can be obtained from the inversion process since the new and the standard coupled-channel calculations lead to different elastic scattering *S* matrices, S_l. This change in S_l can be represented, by inverting S_l for a range of l values, as a change in the effective local elastic scattering potential *V*.

All the required experimental data (elastic, single-2^+, and mutual-2^+ excitations) are available at two energies, $E_{\mathrm{Lab}}=93.8$ MeV and $E_{\mathrm{Lab}}=126.7$ MeV. These are studied with both the conventional and the new inelastic coupling potentials.

In the following section, we review the inversion method. Sections III and IV show the results of the conventional and new coupled-channel calculations, and we present our general conclusions in Sec. V.

II. THE METHOD

We apply the iterative perturbative method for S_l to the $V(r)$ inversion as implemented in the code IMAGO [6]. This method has been described in detail in Refs. [7–13] and relevant points and required definitions are simply noted below. The algorithm iteratively corrects a ''starting reference potential'' (SRP), initially taken here to be the square of the Woods-Saxon potential from Ref. [1]. The quality of the inversion is quantified by the ''phase shift difference'' σ. This is defined in terms of the target *S* matrix S_l^T for which the potential is sought, and the S_l^I as calculated with the potential found by the inversion, as follows:

$$\sigma^2=\sum_l |S_l^T-S_l^I|^2. \tag{1}$$

The minimization of σ usually requires several sequences of inversion iterations in heavy-ion cases as presented here.

III. CONVENTIONAL COUPLING POTENTIAL

We invert the elastic scattering *S*-matrix elements, calculated with the standard coupling potential, at a laboratory energy of 126.7 MeV as follows:

(i) An elastic scattering calculation is carried out without any coupling to excited states of ^{12}C in order to verify that the uncoupled *S* matrix, when inverted, gives precisely the ''bare'' potential. This also verifies that our coupled channel and inversion programs are numerically consistent. The low-order moments (volume integral and rms radius) of the potential obtained in this way are shown in Table I, labeled ''bare.''

(ii) The first excited state (single-2^+) of ^{12}C is included in a coupled-channel calculation in order to observe the effect of the inclusion of this state on the real and imaginary components of the potential. This *S* matrix is inverted and the potential obtained in this way is shown in Table I, labeled ''single.''

TABLE I. Standard coupled-channel calculations. Numerical values of the bare and total inverted potentials (Bare+DPP) obtained by inverting the S matrix at $E_{\mathrm{Lab}}=126.7$ MeV for the single and the mutual cases, where R and I denote the real and the imaginary parts of the potentials and of the radii, respectively.

Case	σ^2	J_{R}	$\langle r^2\rangle_{\mathrm{R}}^{1/2}$	J_{I}	$\langle r^2\rangle_{\mathrm{I}}^{1/2}$
Bare		350.04	4.114	73.301	4.659
Single	1.98×10^{-3}	370.55	4.084	92.67	4.702
Single	1.60×10^{-3}	362.43	4.056	90.84	4.770
Mutual	3.40×10^{-3}	389.54	4.069	103.90	4.686
Mutual	2.23×10^{-3}	382.96	4.041	113.51	4.666

(iii) Mutual excitation as well as single-2^+ state excitation are included. Initially, inversion fails to give a nonoscillatory potential. Therefore, the single inverted potential is employed as the SRP for inverting the ''mutual'' elastic S matrix, and this does lead to a reasonably smooth potential. Characteristics of the potential obtained in this way are also shown in Table I. In each case, two inverted potentials are presented since oscillatory features tend to appear in the potentials. These potentials are, however, much less oscillatory than the mutual potential found when the bare potential is employed as SRP. In each case, the first listed potential is smooth but gives a less than perfect fit to S_l, while the second fits S_l almost perfectly, albeit with some oscillatory features.

The oscillatory features probably represent l dependence in the ''true'' potential, but are hard to interpret and make the calculation of J and $\langle r^2\rangle^{1/2}$ problematic. It is known that S_l, calculated from smooth but l-dependent potentials, can be well represented by l-independent potentials with oscillatory features. It is also expected from the Feshbach formalism that the DPP will be l dependent to some degree. The oscillatory features are clearly a subject for further study, and here we simply present two alternative fits: ''smooth'' and ''lower σ^2,'' where low σ^2 is defined in Eq. (1).

Since the calculation is for identical bosons, we have S_l for even l only. The inverted potentials are thus less well determined because there is less information to define the potential. It may well be reasonable in future studies of this kind to retain odd l in order to either eliminate spurious oscillatory features or to confirm that they should be present.

The nature of the DPP induced by single-channel coupling emerges from a comparison of the characteristics of the ''bare'' potential (first line in Table I) with those with single-channel coupling (second and third lines). Single-channel coupling in this model induces a DPP with an attractive real component with $\Delta J_{\mathrm{R}}\sim15$ MeV fm^3 and an absorptive imaginary component with $\Delta J_{\mathrm{I}}\sim20$ MeV fm^3. The change in $\langle r^2\rangle_{\mathrm{R}}^{1/2}$ is small but negative, in contrast to the change associated with the new coupling, where, as we shall see in Table II, it is positive, at least for smooth potentials.

The inclusion of mutual excitation has a significant effect on the potentials, as the last two lines in Table I reveal. For the surface region, the comparison of the new SRP and the total inverted potentials obtained for the mutual case are shown in Fig. 1 for different values of σ^2. The total effect of the coupling when mutual excitation is included is to induce a DPP with an attractive real component with $\Delta J_{\mathrm{R}}\sim35$ MeV fm^3 and an absorptive component with $\Delta J_{\mathrm{I}}\sim35$ MeV fm^3. For the real potential in particular, the mutual coupling almost doubles the effect.

TABLE II. New coupled-channel calculations. Numerical values of the bare and total inverted potentials (Bare+DPP) obtained by inverting the S matrix at $E_{\mathrm{Lab}}=126.7$ MeV for the mutual case, where R and I denote the real and the imaginary parts of the potentials and of the radii, respectively.

Case	σ^2	J_{R}	$\langle r^2\rangle_{\mathrm{R}}^{1/2}$	J_{I}	$\langle r^2\rangle_{\mathrm{I}}^{1/2}$
Bare		314.19	3.814	95.815	4.659
Mutual	3.67×10^{-3}	351.40	3.905	110.56	4.865

Two important outcomes have emerged at this stage: (i) the simultaneous mutual excitation of the two nuclei in coupled-channels calculations contributes in a substantial way to the internuclear interaction, and (ii) it is confirmed, as is clearly seen from Table I, that inelastic coupling has a substantial contribution to the real as well as to the imaginary potential. Although this was pointed out long ago [14],

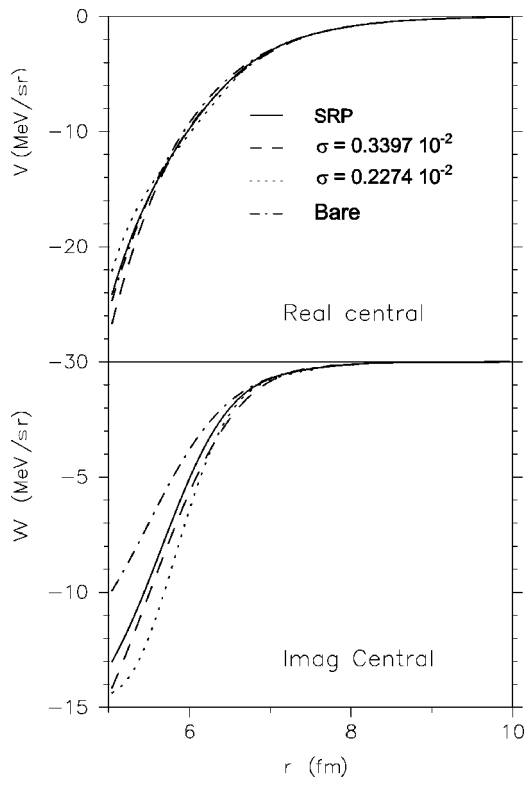

FIG. 1. The comparison of the potentials in the surface region found by inverting the S matrix of the standard coupled-channel calculations at $E_{\mathrm{Lab}}=126.7$ MeV. The long-dashed and the dotted lines correspond to the bottom two lines of Table I with the respective values of σ^2. The dot-dashed lines denote the bare potential, and finally, the solid line is the starting reference potential (SRP) for the mutual case inversion, a smooth solution to the single-case inversion.

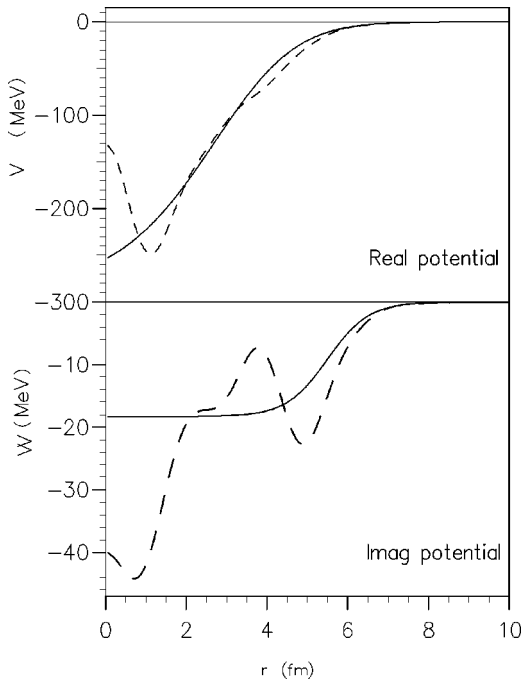

FIG. 2. Comparison of the total inverted potential (long-dashed lines) and the bare potential (solid lines) found by inverting the *S* matrix of the new coupled-channel calculations at $E_{\mathrm{Lab}}=126.7$ MeV. The numerical values are given in Table II.

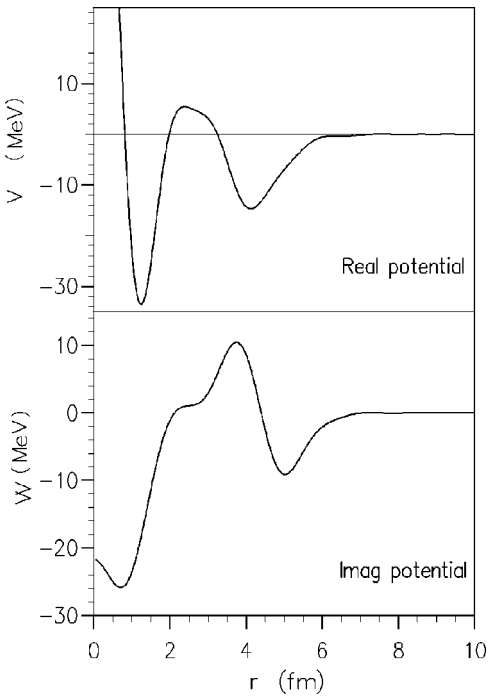

FIG. 3. DPP at $E_{\mathrm{Lab}}=126.7$ MeV found by subtracting the bare potential (solid lines in Fig. 2) from the total inverted potential (long-dashed lines in Fig. 2). The numerical values are given in Table II.

one still often encounters the statement that inelastic coupling just gives rise to additional absorption.

IV. THE DPP WITH THE NEW COUPLING POTENTIAL

We now present the results of inverting the elastic scattering *S* matrix arising from coupled-channel calculations involving the new coupling potential. The numerical characteristics of the potentials are shown in Table II for $E_{\mathrm{Lab}}=126.7$ MeV and in Table III for $E_{\mathrm{Lab}}=93.8$ MeV. The bare potential and the total inverted potential are compared in Fig. 2. The new coupling potential leads to a deepening in the surface region, which can be compared with the effect of the conventional coupling inferred from Fig. 1. This deepening is quantified in Table II where we find that $\Delta J_{\mathrm{R}}\sim 35$ MeV fm^3 and $\Delta J_{\mathrm{I}}\sim 15$ MeV fm^3.

In contrast to the case with the conventional coupling, the added attraction is much greater than the added absorption. It is well known that light heavy-ion reactions are extremely sensitive to the shape of the potential in the surface region. This deepening in the surface region certainly has substantial effects on scattering since it has solved many of the underlying problems of the ^{12}C+^{12}C reaction. Just why the added attraction is much greater than the added absorption with the new coupling interaction (and not with the standard coupling interaction) is among the many properties of the DPP, which are at present not well understood. It presents a challenge for future studies.

Nevertheless, it could be argued that this deepening may be interpreted in terms of the strongly deformed structure of the target nucleus and, as Boztosun and Rae [1] argued, it may be related to the superdeformed state of the ^{24}Mg by considering its two ^{12}C cluster structure (Fig. 3).

The minimum in the surface region and the strongly deformed structure of the target nucleus appear to be related. When one looks at the potential of the ^{16}O+^{28}Si elastic scattering calculations of Kobos and Satchler [15] and Kobos, Satchler, and Mackintosh [16], a minimum in the surface region is observed. In those calculations, a deep double-folding real potential has been used with two small *ad hoc* potentials introduced artificially, and they create the minimum in the surface region. Neither Kobos and Satchler nor others were able to fit the data without two small *ad hoc* potentials.

On the other hand, Boztosun and Rae [2] have also analyzed this reaction from 29 MeV to 142.5 MeV with the new coupling potential and successfully removed these two small *ad hoc* potentials by including the single-2^+ and single-4^+

TABLE III. New coupled-channel calculations. Numerical values of the bare and total inverted potentials (Bare+DPP) obtained by inverting the S-matrix at $E_{\mathrm{Lab}}=93.8$ MeV for the mutual case for different values of σ^2. *R* and *I* denote the real and the imaginary parts of the potentials and of the radii, respectively.

Case	σ^2	J_{R}	$\langle r^2\rangle_{\mathrm{R}}^{1/2}$	J_{I}	$\langle r^2\rangle_{\mathrm{I}}^{1/2}$
Bare		319.34	3.897	94.929	4.757
Mutual	1.50×10^{-3}	356.73	3.919	123.53	5.099
Mutual	1.14×10^{-3}	337.43	3.781	113.72	5.227
Mutual	1.44×10^{-3}	357.88	3.927	123.84	5.099

excited states of the target nucleus ^{28}Si. Kobos and Satchler interpreted their effects in terms of the ''barrier/internal'' wave decomposition. However, the present inversion results imply that the minima in the phenomenological potentials represent inelastic coupling effects. Therefore, as we pointed out, this phenomenon is likely to be related to the deformation of the target nucleus ^{28}Si.

The whole procedure was also applied at 93.8 MeV in order to verify the effect of the new coupling interaction on the elastic scattering potential. Inversion proved to be less straightforward at the lower energy, and problems are encountered in getting a smooth potential with the mutual case. This is partly due to the smaller number of partial waves contributing to the inversion, and also, possibly, due to an increased l dependence at the lower energy. Once more, a number of solutions are presented, with those having lower σ^2 generally corresponding to more oscillatory potentials.

The numerical values of the bare and the total inverted potentials are shown in Table III. The first and third solutions are much smoother than the second, which, however, has a notably lower σ^2.

For the smooth potentials, we have $\Delta J_R \sim 38$ MeV fm^3 and $\Delta J_I \sim 28$ MeV fm^3. Thus, as at 126.7 MeV, the effect on the real part is greater than that on the imaginary part in absolute, though not in relative, terms. The different radial form of the DPP results in a tendency for $\langle r^2 \rangle^{1/2}$ to increase, at least for the smooth solutions. This is a departure from what happens with ''conventional'' coupling and deserves investigation.

V. SUMMARY AND DISCUSSION

The considerable success of the new coupling potential of Boztosun and Rae [1] has subjected the standard coupled-channel procedure to scrutiny. Studies using this new coupling potential may lead to new insights into the formalism and a new interpretation of a class of direct reactions. Here we have investigated the effect of this new coupling potential upon the effective elastic scattering potential by inverting the elastic S matrix derived from coupled-channel calculations. We have observed that the inclusion of the excited states of the target nucleus has an important effect on the real as well as the imaginary potential.

With the standard coupling, interaction, the added attraction is almost the same as the added absorption. However, with the new coupling interaction, the added attraction is much greater than the added absorption. This deep attraction creates a deepening in the surface region for the total inverted potential as shown in Fig. 2, and this solves many of the underlying problems of the ^{12}C+^{12}C, ^{12}C+^{24}Mg, and ^{16}O+^{28}Si systems over a very wide energy range [2–5]. With the standard coupling potential, $\langle r^2 \rangle^{1/2}_{R,I}$, R_{rms} tends to decrease, but with the new coupling it tends to increase. Understanding why R_{rms} increases with the new, but not with the standard, coupling potential is a challenge for further studies. For unstable nuclei, elastic scattering is a source of nuclear size information, so an understanding of how inelastic processes modify $\langle r^2 \rangle^{1/2}$ is important.

ACKNOWLEDGMENTS

The authors wish to thank Dr. W. D. M. Rae, Dr. Y. Nedjadi, Dr. S. Ait-Tahar, Dr. B. Buck, Dr. A. M. Merchant, and Professor B. R. Fulton for valuable discussions and encouragements.

[1] I. Boztosun and W. D. M. Rae, Phys. Rev. C **63**, 054607 (2001); in *Proceedings of the Seventh International Conference on Clustering Aspects of Nuclear Structure and Dynamics*, edited by M. Korolija, Z. Basrak, and R. Caplar (World Scientific, Singapore, 2000), p. 143.
[2] I. Boztosun and W. D. M. Rae, Phys. Rev. C **65**, 024603 (2002).
[3] I. Boztosun and W. D. M. Rae, Phys. Rev. C **64**, 054607 (2001).
[4] I. Boztosun and W. D. M. Rae, Phys. Lett. B **518**, 229 (2001).
[5] I. Boztosun, Phys. Rev. C **66**, 024610 (2002); D. Phil. thesis, Oxford University, 2000; Phys. At. Nucl. **65**, 607 (2002).
[6] S. G. Cooper and R. S. Mackintosh, Report No. OUPD9201.
[7] S. Ait-Tahar, S. G. Cooper, and R. S. Mackintosh, Nucl. Phys. **A561**, 285 (1993).
[8] S. Ait-Tahar, S. G. Cooper, and R. S. Mackintosh, Nucl. Phys. **A562**, 101 (1993).
[9] S. G. Cooper and R. S. Mackintosh, Nucl. Phys. **A513**, 373 (1990).
[10] S. G. Cooper, M. A. McEwan, and R. S. Mackintosh, Phys. Rev. C **45**, 770 (1992).
[11] S. G. Cooper and R. S. Mackintosh, Phys. Rev. C **54**, 3133 (1996).
[12] G. H. Rawitscher, D. Lukaszek, R. S. Mackintosh, and S. G. Cooper, Phys. Rev. C **49**, 1621 (1994).
[13] R. S. Mackintosh and A. M. Kobos, Phys. Lett. **116B**, 95 (1982).
[14] R. S. Mackintosh, Nucl. Phys. **A164**, 398 (1971); R. S. Mackintosh and A. A. Ioannides, *Advanced Methods in Analysis of Nuclear Scattering Data* (Springer, Berlin, 1985), p. 283.
[15] A. M. Kobos and G. R. Satchler, Nucl. Phys. **A427**, 589 (1984).
[16] A. M. Kobos, G. R. Satchler, and R. S. Mackintosh, Nucl. Phys. **A395**, 248 (1983).